Dynamic change in the photoconductivity sign in *n*-Ge in intense submillimeter radiation

S. D. Ganichev, S. A. Emel'yanov, and I. D. Yaroshetskiĭ
A. F. Ioffe Physicotechnical Institute, Academy of Sciences of the USSR, Leningrad

(Submitted 3 August 1983; resubmitted 7 September 1983)
Pis'ma Zh. Eksp. Teor. Fiz. **38**, No. 8, 370–373 (25 October 1983)

A dynamic change in the sign of the intraband photoconductivity has been observed in *n*-Ge: The sign of the photoconductivity changes during the exciting light pulse. The effect is linked with a change caused in the momentum relaxation mechanism by a heating of the electron gas.

PACS numbers: 72.40. + w, 72.80.Cw, 78.70.Gq

We have observed and studied a dynamic change in the sign of the intraband conductivity in *n*-Ge.

The electron density in the test samples ranged from 5×10^{14} to 2.2×10^{16} cm^{-3} at $T_0 = 78$ K and 300 K. The intraband excitation of the semiconductor was caused by the beam at a wavelength of 90.55 μm from a pulsed NH_3 laser optically pumped by a CO_2 laser.[1,2] The intensity of the submillimeter radiation was varied up to 4 MW/cm^2. The half-width of the output pulse was 4×10^{-8} s.

We found that the shape of the photoconduction pulse and the corresponding time dependence of the magnitude and sign of the intraband photoconductivity depend on the excitation intensity (Fig. 1). At relatively low incident intensities I (Fig. 1a) the shape of the pulse is precisely the same as that of the laser pulse, while its sign corre-

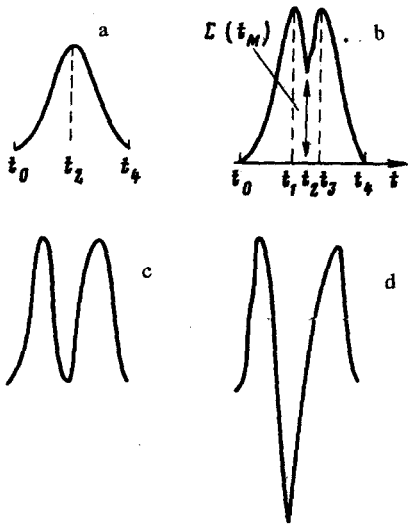

FIG. 1. Change in the shape of the intraband photoconductivity pulse with increasing radiation intensity. $N_d = 7\times10^{15}$ cm^{-3}, $T_0 = 78$ K. a—$I = 0.01I^*$; b—$I = 0.01I^*$; c—$I = 0.25I^*$; d—$I = I^* = 4$ MW/cm^2.

sponds to a positive intraband photoconductivity. As I is increased, the shape of the photoconduction pulse changes (Fig. 1b). In the initial part of the pulse, up to the time t_1, the increase in the instantaneous value of $I(t)$ is accompanied by an increase in the signal corresponding to the relative intraband photoconductivity, $\Delta\sigma/\sigma_0 = \Sigma(t)$, but then $\Sigma(t)$ starts to fall while the radiation intensity continues to rise. This behavior continues until t_2, at which point $I(t)$ reaches a maximum; then the radiation intensity decreases, while the photoconductivity increases and continues to do so until time t_3. After this point, the decrease in $I(t)$ is accompanied by a decrease in the photoconduction signal. In the situation shown in Fig. 1b, the photoconductivity $\Sigma(t_M)$ corresponding to the maximum intensity of the laser pulse, I_M at the time $t_2 = t_M$, is lower than the photoconductivity at (for example) the time t_1. As the incident intensity is raised further, we find a situation in which $\Sigma(t_M)$ becomes zero (Fig. 1c), and at even higher I we see a change in the sign of $\Sigma(t_M)$ (Fig. 1d). In this experiment, we might note, the magnitude $|\Sigma(t_M)|$ came to exceed $|\Sigma(t_1)|$ and $|\Sigma(t_3)|$ by as much as two orders of magnitude. The I dependence of the shape of the photoconduction pulse described above corresponds to n-Ge samples at $T_0 = 78$ K with a density above 1.8×10^{15} cm^{-3}. At lower densities or at $T_0 = 300$ K, the photoconduction pulse has no structural features and reproduces the shape of the laser pulse; the intraband photoconductivity $\Sigma(t)$ is negative. Figure 2 shows the dependence $\Sigma(t_M) = f(I)$ for samples with various carrier densities n_0. We see that at low values of n_0 (curve 1) the intraband photoconductivity is negative over the entire I range, while at higher values of n_0 (curves 2–4) the photoconductivity $\Sigma(t_M)$ is initially positive but then drops to zero and ultimately changes sign, becoming negative at large values of I. The intensity I_M^0 at which $\Sigma(t_M)$ vanishes is very sensitive to n_0.

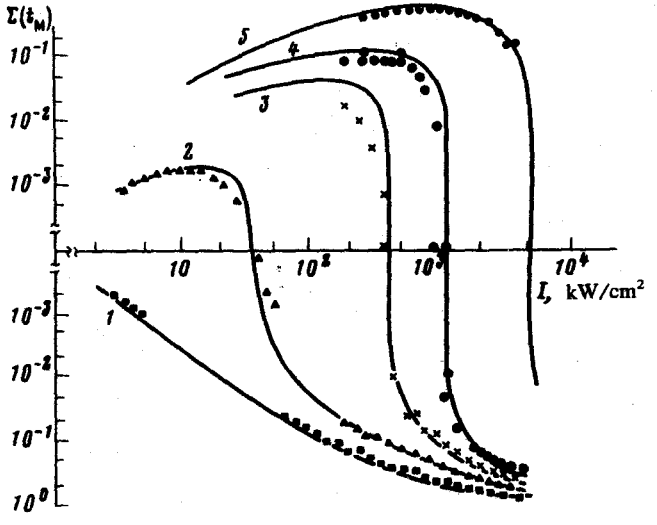

FIG. 2. Dependence of the mobility on the radiation intensity. $T_0 = 78$ K. 1—$N_d = 5\times10^{14}$ cm^{-3}; 2—$N_d = 2.1\times10^{15}$ cm^{-3}; 3—$N_d = 4\times10^{15}$ cm^{-3}; 4—$N_d = 7\times10^{15}$ cm^{-3}; 5—$N_d = 2.2\times10^{16}$ cm^{-3}. Points—experimental; curves—theoretical.

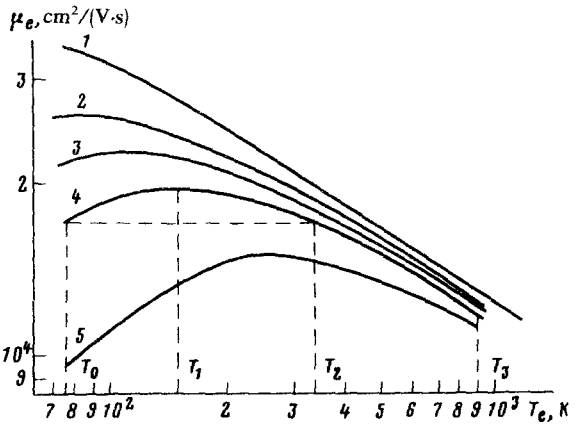

FIG. 3. Mobility as a function of the electron temperature. $T_0 = 78$ K. 1—$N_d = 5\times10^{14}$ cm^{-3}; 2—$N_d = 2.1\times10^{15}$ cm^{-3}; 3—$N_d = 4\times10^{15}$ cm^{-3}; 4—$N_d = 7\times10^{15}$ cm^{-3}; 5—$N_d = 2.2\times10^{16}$ cm^{-3}.

Analysis shows that the dynamic change observed in the sign of the intraband photoconductivity results from a substantial heating of the electron gas by the radiation, the resulting change in the momentum relaxation of the charge carriers, and, ultimately, the resulting change in their mobility μ_e. The situation can be understood with the help of Fig. 3, which shows μ_e as a function of the electron temperature T_e according to calculations incorporating scattering by ionized impurities and by acoustic phonons.[1)] The temperature T_e is in turn a function of the radiation intensity I. It can be seen from Fig. 3 that at comparatively low impurity densities N_d the scattering is primarily a scattering by acoustic phonons, and μ_e falls off with increasing T_e (curve 1), in turn causing a negative photoconductivity $\Sigma(t)$, since $\Sigma(t) = \Delta\sigma/\sigma_0 = \Delta\mu/\mu_0 = (\mu_e - \mu_0)/\mu_0$, where μ_0 is the mobility at the lattice temperature T_0. With increasing T_e, the magnitude of the negative photoconductivity increases. An increase in N_d has the effect of causing the contribution of the ionized impurities to the momentum scattering to become important when T_e is not greatly different from T_0 ($T_0 = 77$ K). In this case, as the electron temperature T_e increases, the mobility $\mu_e(T_e)$ initially does not fall off but instead increases (curves 2-5 in Fig. 3), so that $\Sigma(t)$ is positive. Later, however, the scattering by acoustic phonons becomes predominant, so that again μ_e decreases with increasing T_e (the descending parts of curves 2-5 in Fig. 3). As can be seen from (for example) curve 4 in Fig. 3, $\Sigma(t)$ is positive and increases as T_e varies from T_0 to T_1; between T_1 and T_2, $\Sigma(t)$ drops to zero; finally, between T_2 and T_3, $\Sigma(t)$ changes sign, becoming negative. If the laser pulse is approximately bell-shaped, this behavior prevails throughout the rising part of the pulse (its leading edge). During the decay of the radiation intensity (on the trailing edge) all the events described above occur again, in the opposite order. Figure 1 shows some corresponding oscilloscope traces.

Figure 2 shows curves of $\Sigma(t) = f(I)$ calculated for various carrier densities from the balance equation[3] with allowance for the energy loss due to acoustic and optical phonons. We see that there is a good agreement between the experimental and theoretical results.

We thank I. N. Yassievich for a discussion of these results.

[1)]Estimates based on the known interaction constants show that in this case the scattering by optical strain phonons plays a minor role. Since the characteristic time for electron-electron collisions is much shorter than all other characteristic times in our case, we have adopted the approximation of an electron temperature.

---

[1]S. D. Ganichev, S. A. Emel'yanov, and I. D. Yaroshetskiĭ, Pis'ma Zh. Eksp. Teor. Fiz. **35**, 297 (1982) [JETP Lett. **35**, 368 (1982)].
[2]S. D. Ganichev, S. A. Emel'yanov, and I. D. Yaroshetskiĭ, Pis'ma Zh. Eksp. Teor. Fiz. **37**, 479 (1983) [JETP Lett. **37**, 568 (1983)].
[3]E. M. Conwell, High Field Transport in Semiconductors, Academic, New York (1967) (Russ. transl. Mir, Moscow, 1970).

Translated by Dave Parsons
Edited by S. J. Amoretty